Remote sensing of the solar photosphere: a tale of two methods

IOP Conf. Series: Journal of Physics: Conf. Series **956** (2018) 012006 doi:10.1088/1742-6596/956/1/012006

Remote sensing of the solar photosphere: a tale of two methods

G Viavattene[1], F Berrilli[1], M Collados Vera[2], D Del Moro[1], L Giovannelli[1], B Ruiz Cobo[2] and F Zuccarello[3]

[1] Università di Roma "Tor Vergata", Via della Ricerca Scientifica, I-00133 Roma, Italy
[2] Instituto de Astrofisica de Canarias, Calle Vìa Làctea, s/n, 38205 San Cristòbal de La Laguna, Tenerife, Spain
[3] Università degli Studi di Catania, Dipartimento di Fisica e Astronomia, Via Santa Sofia 78, 95123 Catania, Italy

E-mail: giorgio.viavattene@roma2.infn.it

Abstract. Solar spectro-polarimetry is a powerful tool to investigate the physical processes occurring in the solar atmosphere. The different states of polarization and wavelengths have in fact encoded the information about the thermodynamic state of the solar plasma and the interacting magnetic field. In particular, the radiative transfer theory allows us to invert the spectro-polarimetric data to obtain the physical parameters of the different atmospheric layers and, in particular, of the photosphere. In this work, we present a comparison between two methods used to analyze spectro-polarimetric data: the classical Center of Gravity method in the weak field approximation and an inversion code that solves numerically the radiative transfer equation. The Center of Gravity method returns reliable values for the magnetic field and for the line-of-sight velocity in those regions where the weak field approximation is valid (field strength below 400 G), while the inversion code is able to return the stratification of many physical parameters in the layers where the spectral line used for the inversion is formed.

1. Introduction

The interaction between magnetic fields and convection in the solar photosphere regulates a large variety of physical processes that we can observe from Earth with ground-based solar telescopes. One of the challenges of the modern solar physics is to measure very precisely the magnetic field and the thermodynamical properties of the solar photosphere exploiting the polarization of the light, which encodes all this information. In fact, by analyzing the polarization state of the electromagnetic radiation at different wavelengths, we are able to extract the magnetic fields in some layers of the solar photosphere harnessing the radiative transfer and the Zeeman effect theories. Therefore, the Radiative Transfer Equation (RTE) is at the core of this approach. There are different methods and approximations to solve it: there are analytical solutions of the RTE based on several assumptions and there are numerical solutions which, using more realistic atmospheric models, return more information about the physical parameters of the atmosphere. In this work, we present some results obtained using two different methods, applied to interpret spectro-polarimetric observations of the so-called Quiet Sun [1]. We compare the results from the Center of Gravity (CoG) method [2–4], based on weak field approximation and an analytical solution of the RTE, and the NICOLE inversion technique [5,6] which solves numerically the RTE.

2. The radiative transfer

The propagation of the electromagnetic radiation through a stellar atmosphere is a complex, non-linear, three dimensional and time dependent problem, that involves the properties of the whole atmosphere. The RTE describes how the radiation propagates through the solar atmosphere:

$$\frac{d\mathbf{I}}{d\tau_c} = \mathbf{K}(\mathbf{I} - \mathbf{S}) \tag{1}$$

where $\mathbf{I} = (I, Q, U, V)^T$ is the Stokes polarization vector (I is the intensity, Q and U are connected to the linear polarization, and V is connected to the circular polarization), $\tau_c = \int_s^{s_{lim}} \chi_{cont}\, ds$ is the continuum optical depth (χ_{cont} is the continuum opacity and s_{lim} is the geometrical distance corresponding to $\tau_c = 0$), $\mathbf{K}$ is the 4×4 propagation matrix and $\mathbf{S}$ is the source function. In the Non Local Thermodynamic Equilibrium (NLTE) approach the RTE is a set of four coupled differential equations and, in order to solve the problem, we have to consider both the radiative and the collisional transitions. Only numerical solutions exist and they require an iterative procedure to be found. In the following, we examine two approximations that are used to solve analytically the RTE.

2.1. The Milne-Eddington approximation

In the Milne-Eddington (ME) approximation the propagation matrix is constant with respect to the optical depth and it is the same at all the wavelengths, while the source function depends linearly on the continuum optical depth. A constant propagation matrix implies that all the parameters that define the spectral line formation (i.e. the line-to-continuum absorption coefficient, the Doppler width and the damping parameter) are constant and also that the magnetic field vector $\mathbf{B}$ and the velocity along the line-of-sight $v_{\rm los}$, are constant through the atmosphere. Therefore, in the ME approximation the physical parameters are not stratified along the atmosphere. In this approximation the $\mathbf{K}$ matrix, and so the analytical solution, are connected with just nine parameters of the atmosphere: three for the magnetic field vector (the intensity, the inclination along the line-of-sight and the azimuth angle); two for the source function (the constant and the linear terms); three for the shape of the spectral line (the line-to-continuum absorption coefficient, the Doppler width and the damping parameter); and one for the velocity along the line-of-sight $v_{\rm los}$. Thus, assuming these nine parameters and using the RTE, we can obtain *synthetic* Stokes profiles (i.e. the full polarization state with respect to wavelength). On the contrary, starting from the observed Stokes profiles, we can extract the atmospheric parameters, by the process called *inversion*. It is worth stressing that such a simple atmosphere produces only very simple Stokes profiles.

2.2. The weak field approximation and the Center of Gravity method

Another approximation to solve the RTE is the weak field approximation, which assumes the magnetic field to be constant with respect to the optical depth and below a few hundreds of Gauss. Under such hypotheses, the amplitude of the Stokes V lobes is proportional to the magnetic field intensity. The CoG method [2–4] assumes these hypotheses and allows us to evaluate the component of the magnetic field intensity along the line-of-sight (longitudinal component) using this equation:

$$B_{||} = B\cos\chi = \frac{1.071 \times 10^9}{\bar{g}\lambda_0^2}(\lambda_+ - \lambda_-) \tag{2}$$

where $\bar{g}$ is the effective Landé factor, λ_0 is the laboratory wavelength of the observed spectral line, and λ_+ and λ_- are respectively the positions of the positive and negative lobes of a Stokes

V profiles.

3. Inversion techniques

The previous approximations can only describe simple Stokes profiles. Nature is very often more complex than this. In real solar spectro-polarimetric data, asymmetric Stokes profiles are commonly observed and it is necessary to increase the complexity of the atmospheric model in order to match the observations. In fact, the physical parameters of the solar atmosphere vary with the optical depth, and therefore with the geometrical depth. To describe this stratification of the atmospheric parameters, we can discretize the altitude layers of the atmosphere in a grid of point, called *nodes*.

The physical parameters of the solar atmosphere are extracted from the observed Stokes profiles using an inversion technique. In practice, the distance between the observed Stokes profiles and the synthetic ones is computed using a merit function:

$$\chi^2(\mathbf{x}) = \frac{1}{N_f} \sum_{s=0}^{3} \sum_{i=1}^{q} [I_s^{obs}(\lambda_i) - I_s^{syn}(\lambda_i; \mathbf{x})]^2 \, w_{s,i}^2 \tag{3}$$

where $\mathbf{x}$ is a vector containing the whole set of the atmospheric parameters, N_f is the number of nodes used to discretize the model atmosphere (and defines the number of degrees of freedom of the model), s is the index for the four Stokes profiles, i is the index for the wavelengths, and $w_{s,i}$ are weights used to take into account the different signal-to-noise ratios of the Stokes profiles.

Therefore, the purpose of the inversion techniques is to find the synthetic Stokes profiles that best match the observed ones by iteratively minimizing the merit function. These techniques use a stratified atmosphere model and retrieve a best estimate of the solar atmosphere given the measured Stokes parameters and the chosen model. For a more detailed explanation of the operation of the inversion techniques in general, see [7] and [8].

4. Data analysis

The dataset used for the analysis has been acquired on 2006 with the Interferometric BIdimensional Spectropolarimeter (IBIS [9, 10]) located in the Dunn Solar Telescope (DST) at Sacramento Peak, National Solar Observatory (NSO), New Mexico. The spectro-polarimetric dataset of the Quiet Sun consists in observations of the spectral region containing the FeI 6301.5 Å and 6302.5 Å lines, and, pixel by pixel of the Field of View (FoV), the four Stokes profiles are measured by the instrument. The FoV framed by the instrument is 40×40 arcsec^2, which corresponds approximately on the solar surface to 30×30 Mm^2. For more information on the dataset, see [11–13]. In Fig. 1 the spectral scanning of Stokes I and V profiles performed by IBIS instrument are shown.

The dataset has been calibrated with the IBIS pipeline [14]. In Fig. 2 examples of the Stokes I and V maps of the FoV are shown. The spectral position of the Stokes I map is centered in the continuum, while the spectral position of the Stokes V map is centered in the negative lobe of the 6301.5 Å line. In the Stokes I map is clearly visible the photospheric granulation which is associated to the temperature of the solar photosphere; in fact, the central part of the granules is hotter than the surrounding and the intergranular lanes are cooler. In the Stokes V map some coherent magnetic structures are visible. It is interesting to note that these magnetic structures do not exhibit an evident counterpart in the Stokes I map.

The dataset has been analyzed using both NICOLE and CoG methods. The characterizing parameters used for the inversion with NICOLE are: temperature represented with three nodes;

$v_{\rm los}$ represented with two nodes; magnetic field constant with height; no micro-turbulence contribution considered; no macro-turbulence considered, but instrumental spectral profile taken into account; initializing atmosphere model Harvard-Smithsonian Reference Atmosphere [15]. The choice of the number of nodes is a trade-off between the quality of the data and the complexity (number of degrees of freedom) of the model atmosphere which can be retrieved by the inversions. Given the spectral sampling, the signal-to-noise ratio and the number of spectral lines of the dataset, our choice grants an adequate atmosphere stratification without data over-fitting.

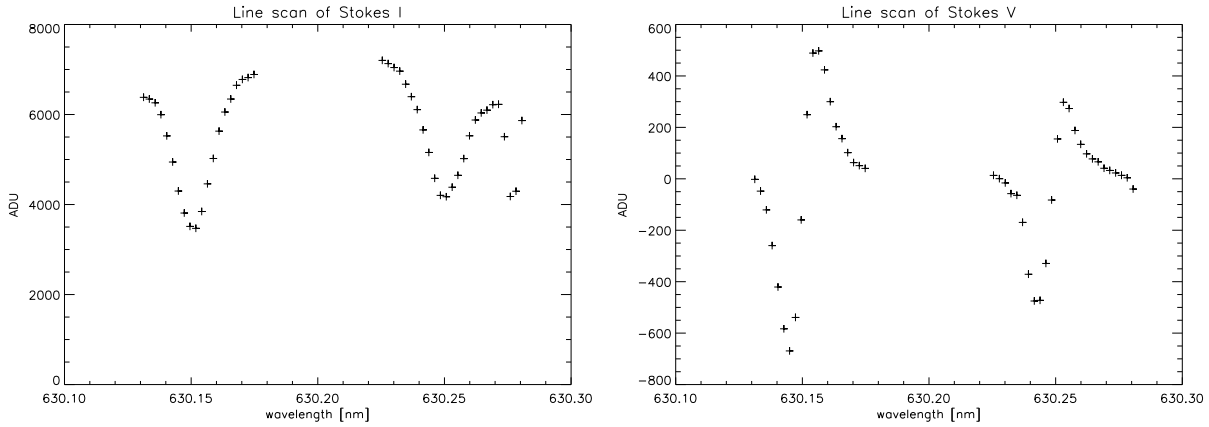

Figure 1. Left panel: IBIS scan of Stokes I profile of Fe I 630.15 nm and 630.25 nm spectral lines. At 630.28 nm is visible a telluric line due to absorption of water in the Earth atmosphere. Right panel: IBIS scan of Stokes V profile of Fe I 630.15 nm and 630.25 nm spectral lines. As expected, the telluric line shows no circular polarization signal. All counts are reported in Analog-Digital Units (ADU).

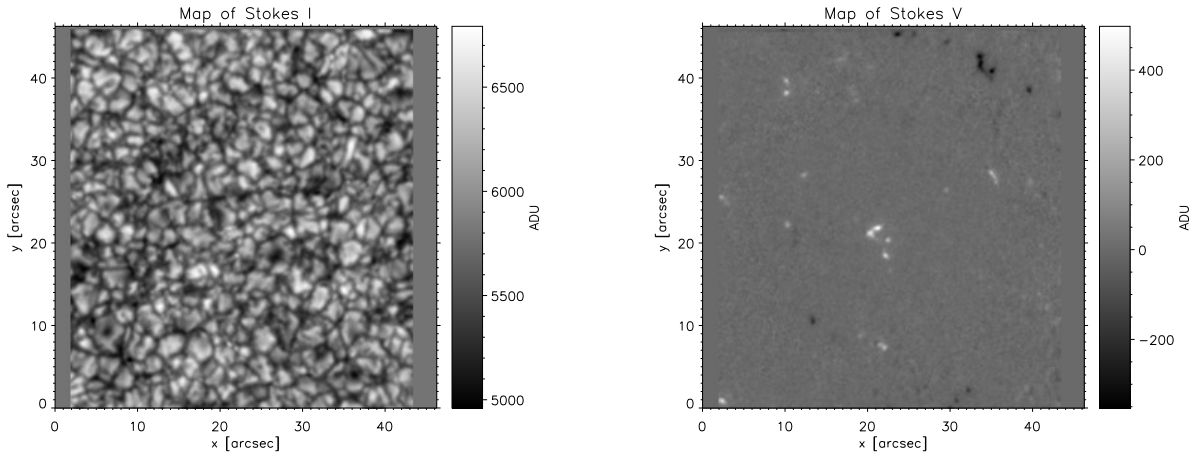

Figure 2. Left panel: Map of Stokes I in the continuum. Right panel: Map of Stokes V in the negative lobe of the 630.15 nm line. Counts are reported in Analog-Digital Units (ADU).

4.1. Comparisons and discussion: the CoG method vs. the inversions

In this subsection we will present the results of the data analysis and some comparisons between the two methods (CoG method and the NICOLE inversion technique). In particular, we focus our attention on the longitudinal component of the magnetic field. For this analysis, the frames with poor seeing are not considered.

An Interactive Data Language (IDL) code has been developed in order to perform the evaluation of the longitudinal component of the magnetic field analyzing the spectro-polarimetric dataset pixel by pixel and using Eq. 2. The values of the longitudinal magnetic field have been obtained also with the NICOLE inversion code. The resulting magnetic field maps of one temporal frame are reported in Fig. 3. It can be noted that both methods retrieve coherent magnetic structures although the analysis has been performed pixel by pixel.

We also compare the Probability Density Functions (PDFs) of the longitudinal magnetic field

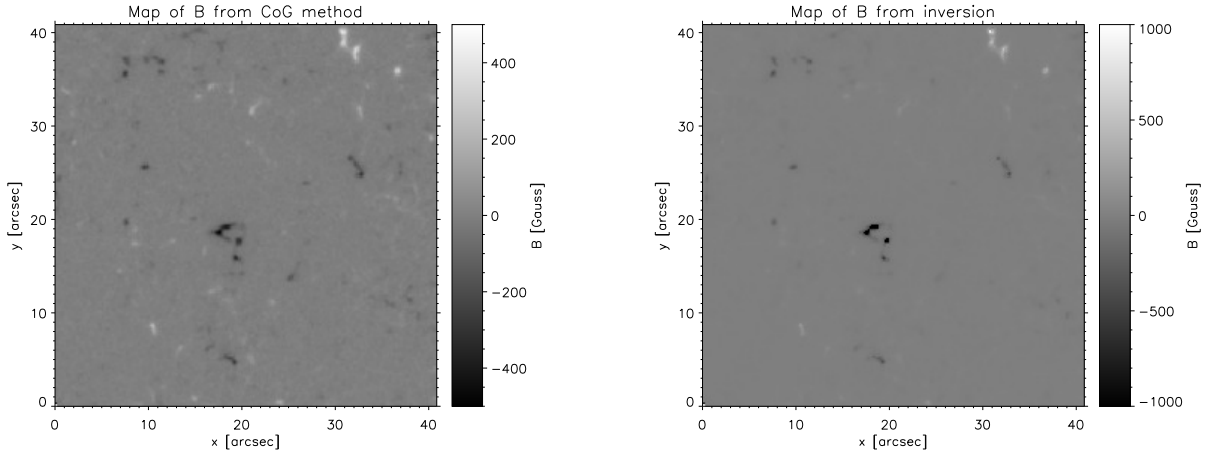

Figure 3. Left panel: Map of the longitudinal component of the magnetic field evaluated with the CoG method. The map is saturated between -500 G (black) and +500 G (white) according to the weak field approximation regime. Right panel: Map of the longitudinal component of the magnetic field evaluated with NICOLE inversions. The map is saturated between -1000 G (black) and +1000 G (white).

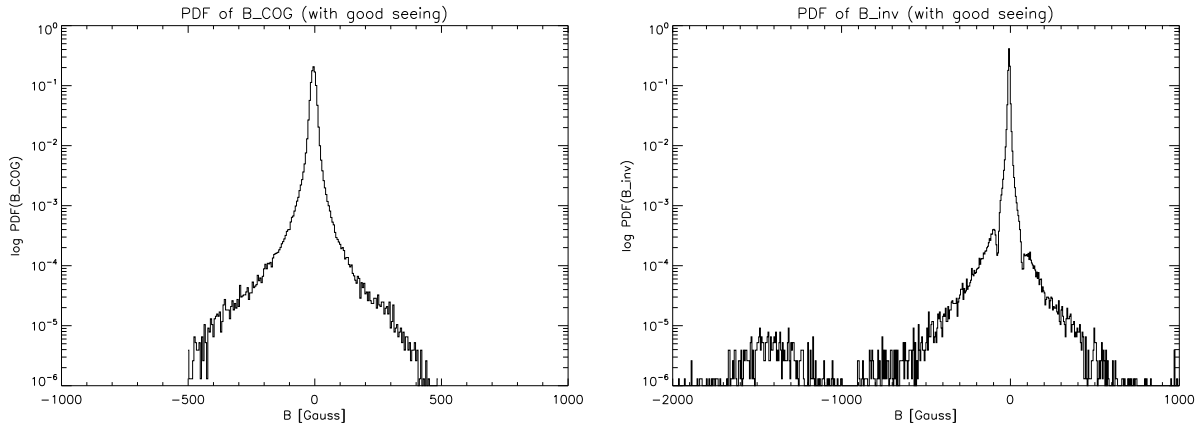

Figure 4. Left panel: PDF of the longitudinal magnetic field evaluated using the CoG method. Right panel: PDF of the longitudinal magnetic field evaluated with inversion techniques.

values retrieved by the two methods. In Fig. 4 (left panel) the PDF of the longitudinal magnetic field evaluated with the CoG method is shown. It can be noted that the wings of the PDF spread out to approximately -500 G and +500 G at most. In fact, for magnetic fields greater than 400 G the weak field approximation fails and the expression in Eq. 2 is not valid anymore, thus producing such a saturation effect in the PDF. Nevertheless, the PDF from the CoG method is quite symmetric. In Fig. 4 (right panel) the PDF of the longitudinal magnetic field evaluated with NICOLE inversions is shown. This PDF is peculiar because, apart from some pixels that have magnetic field values below -1000 G, its central part is not symmetric and two asymmetric bumps are visible. A possible explanation to these features is related to the tendency of inversion techniques to overestimate weak fields: in fact, pixels which should have lower absolute values of magnetic field are shifted by the inversions to higher absolute values, and therefore they contribute to the formation of the two bumps.
In this analysis, pixels with magnetic field values below three times the noise values have been excluded.
Even considering the saturation effect of the CoG method for high magnetic field values, it is evident that the magnetic field retrieved by NICOLE is systematically larger than the one retrieved by the CoG. This effect has also been discussed in [16]. As of today, improving reliability of the inversion retrievals in the weak field range is a very dynamic field of research.

5. Conclusion

We conclude by summarizing the principal advantages and disadvantages of the two methods which have been used to analyze the spectro-polarimetric data.
On one hand, the inversion technique requires long computation time, is able to retrieve the stratification of the physical parameters along the solar atmosphere, but tends to overestimate weak magnetic fields. On the other hand, the CoG method has more assumptions and returns an analytical result in a very short computational time. It retrieves a value of the longitudinal magnetic field (as well as of the line-of-sight velocity) "averaged" along the atmospheric layers which mostly contribute to the observed spectral line shape.

References

[1] Del Moro D 2004 *Astronomy & Astrophysics* **420** 1007
[2] Semel M D 1967 *Annales d'Astrophysique* **30** 513
[3] Rees D E and Semel M D 1979 *Astronomy & Astrophysics* **74** 1R
[4] Landi Degl'Innocenti E and Landolfi M 2004 *Astrophysics and Space Science Library* **307** L
[5] Socas-Navarro H, de la Cruz Rodríguez J, Asenzio Ramos A, Trujillo Bueno J and Ruiz Cobo B 2015 *Astronomy & Astrophysics* **577** 7
[6] Socas-Navarro H 2015 *Astrophysics Source Code Library* ascl:1508.002
[7] Ruiz Cobo B and del Toro Iniesta J C 1992 *The Astrophysical Journal* **398** 375
[8] Ruiz Cobo B and del Toro Iniesta J C 1994 *Astronomy & Astrophysics* **283** 129
[9] Cavallini F, Berrilli F, Cantarano S and Egidi A 2001 *Mem. SAIt* **72** 554
[10] Cavallini F 2006 *Solar Physics* **236** 415
[11] Viticchié B, Del Moro D, Berrilli F, Bellot Rubio L and Tritschler A 2009 *Astrophysical Journal* **700** L145
[12] Del Moro D, Giannattasio F, Berrilli F, Consolini G, Lepreti F and Gošić M 2015 *Astronomy & Astrophysics* **576** A47
[13] Del Moro D, Giovannelli L, Pietropaolo E and Berrilli F 2017 *Experimental Astronomy* **43** 23
[14] Viticchié B, Del Moro D, Criscuoli S and Berrilli F 2010 *The Astrophysical Journal* **273** 787
[15] Gingerich O, Noyes R W, Kalkofen W and Cuny Y 1971 *Solar Physics* **18** 347
[16] del Toro Iniesta J C and Ruiz Cobo B 2016 *Living Review in Solar Physics* **13** 1 4 84 pp.